The Astrophysical Journal Letters, 812:L25 (6pp), 2015 October 20 doi:10.1088/2041-8205/812/2/L25

AS ABOVE, SO BELOW: EXPLOITING MASS SCALING IN BLACK HOLE ACCRETION TO BREAK DEGENERACIES IN SPECTRAL INTERPRETATION

Sera Markoff[1], Michael A. Nowak[2], Elena Gallo[3], Robert Hynes[4], Jörn Wilms[5], Richard M. Plotkin[3], Dipankar Maitra[6], Catia V. Silva[1,7], and Samia Drappeau[8]
[1] Anton Pannekoek Institute for Astronomy, University of Amsterdam, 1098 XH Amsterdam, The Netherlands; S.B.Markoff@uva.nl, C.V.DeJesusSilva@uva.nl
[2] Massachusetts Institute of Technology, Kavli Institute for Astrophysics, Cambridge, MA 02139, USA; mnowak@space.mit.edu
[3] Department of Astronomy, University of Michigan, Ann Arbor, MI 48109-1042, USA; egallo@umich.edu
[4] Department of Physics and Astronomy, Louisiana State University, Baton Rouge, LA 70803-4001, USA; rih@redstick.phys.lsu.edu
[5] Dr. Karl Remeis-Sternwarte & ECAP, Universität Erlangen-Nürnberg, D-96049 Bamberg, Germany; joern.wilms@sternwarte.uni-erlangen.de
[6] Department of Physics and Astronomy, Wheaton College, Norton, MA 02766, USA; maitra_dipankar@wheatoncollege.edu
[7] SRON Netherlands Institute for Space Research, 3584 CA, Utrecht, The Netherlands
[8] CNRS, IRAP, BP 44346, F-31028 Toulouse cedex 4, France; samia.drappeau@irap.omp.eu
Received 2015 August 3; accepted 2015 September 27; published 2015 October 14

ABSTRACT

Over the past decade, evidence has mounted that several aspects of black hole (BH) accretion physics proceed in a mass-invariant way. One of the best examples of this scaling is the empirical "fundamental plane of BH accretion" relation linking mass, radio, and X-ray luminosity over eight orders of magnitude in BH mass. The currently favored theoretical interpretation of this relation is that the physics governing power output in weakly accreting BHs depends more on relative accretion rate than on mass. In order to test this theory, we explore whether a mass-invariant approach can simultaneously explain the broadband spectral energy distributions from two BHs at opposite ends of the mass scale but that are at similar Eddington accretion fractions. We find that the same model, with the same value of several fitted physical parameters expressed in mass-scaling units to enforce self-similarity, can provide a good description of two data sets from V404 Cyg and M81*, a stellar and supermassive BH, respectively. Furthermore, only one of several potential emission scenarios for the X-ray band is successful, suggesting it is the dominant process driving the fundamental plane relation at this accretion rate. This approach thus holds promise for breaking current degeneracies in the interpretation of BH high-energy spectra and for constructing better prescriptions of BH accretion for use in various local and cosmological feedback applications.

Key words: accretion, accretion disks – black hole physics – galaxies: active – galaxies: jets – radiation mechanisms: non-thermal – X-rays: binaries

1. INTRODUCTION

Accreting black holes (BHs), whether in Galactic X-ray binaries (BHBs) or active galactic nuclei (AGNs), drive a complicated system of inflowing (quasi-)thermalized plasma in an accretion disk, outflowing plasma in the form of winds and/or relativistic jets, and a hot corona that may comprise elements of both phenomena (see, e.g., Markoff et al. 2005). The basic morphological similarities between these systems have led to the proposal that at least some general properties of BH accretion might scale predictably with mass, regardless of outer boundary conditions (i.e., fueling).

Over the past decade, there has been increasing evidence of such a mapping between BHB accretion states (McClintock & Remillard 2006; Belloni 2010) and AGN classifications (e.g., Körding et al. 2006b). The two most compelling examples are the correspondences between variability timescales in BHBs and AGNs (e.g., McHardy et al. 2006, 2007) and the fundamental plane of BH activity (hereafter FP) discovered over a decade ago (Merloni et al. 2003; Falcke et al. 2004) and increasingly refined via several newer studies (e.g., Körding et al. 2006a; McHardy et al. 2006; Gültekin et al. 2009; Plotkin et al. 2012).

The FP is an empirical relation between the radio and X-ray luminosities and masses of accreting BHs in the "hard" BHB state associated with compact, self-absorbed jets (see Fender 2001; McClintock & Remillard 2006) and low-luminosity AGNs with jet cores: i.e., LLAGNs in LINERS and FRI/BL Lacertae objects. Essentially all weakly accreting AGNs with jets seem to adhere to this plane. The planar coefficients can be derived assuming a common reservoir of accretion power linearly dependent on accretion rate $\dot{m}$ (expressed in mass-scaling Eddington units $\dot{m} = \dot{M}/\dot{M}_{\rm Edd}$, where $\dot{M}_{\rm Edd} = L_{\rm Edd}/(0.1c^2)$ and $L_{\rm Edd} = 4\pi GMm_pc/\sigma_T$), injected into a region whose size scales linearly with $M_{\rm BH}$, together with conservation laws, optical depth effects, and low radiative efficiencies ($L \propto \dot{m}^q$, where $q \approx 2$; Falcke & Biermann 1995; Heinz & Sunyaev 2003; Markoff et al. 2003; Plotkin et al. 2012). The actual physics driving the FP is not yet fully understood, primarily because of persistent degeneracy in the interpretation of the spectral energy distributions (SEDs). Both synchrotron radiation as well as synchrotron self-Compton (SSC) in several flavors of radiatively inefficient accretion flows (RIAFs; Narayan & Yi 1994; Yuan et al. 2003) or outflows (e.g., Markoff et al. 2005; Yuan et al. 2005) have radiative efficiencies consistent with the limits set by the FP ($q \approx 2$; though see Plotkin et al. 2012).

The FP predicts that BHs regulate their power output similarly when at similar relative accretion rates (see, e.g., Heinz & Sunyaev 2003; Markoff 2010 for a broader review). In other words, two sources at similar $\dot{m}$ should radiate from regions of similar size (in gravitational radii $r_{\rm g} \equiv GM/c^2$) and with the same physical mechanism (or at least mechanisms with the exact same efficiencies). This Letter explores a new approach to quantitatively test this assumption, with an eye toward breaking the degeneracy between synchrotron and SSC models, via the joint modeling of broadband SEDs from

two BHs at extreme ends of the mass scale. In Section 2, we describe the methodology and briefly summarize the model we use for this study. In Section 3, we present our results, and in Section 4, we conclude with an outlook for potential extensions of this approach.

2. SUMMARY OF MODEL AND METHODOLOGY

The low-energy spectrum of FP BHs consists of a flat/inverted synchrotron component, associated with self-absorbed emission from stratified regions along a compact jet (e.g., Blandford & Königl 1979). The X-ray bands often show evidence of weak emission from a thermal accretion disk (e.g., Shakura & Sunyaev 1973; Mitsuda et al. 1984) plus a non-thermal component over which debate rages as to the relative contributions of synchrotron and inverse-Compton processes. Real-time radio/X-ray correlations in BHBs clearly demonstrate that the jets and the X-ray source are tightly coupled over orders of magnitude in luminosity. A mass-dependent normalization extends this relation to AGNs, defining the FP.

A straightforward test can isolate the mass-dependent effects: express a given model in terms of mass-scaling units (i.e., all distances expressed in r_g and power in units of $L_{\rm Edd} = 1.25 \times 10^{38} (M/M_\odot)$ erg s^{-1}), and see how it fares when applied to data from stellar to supermassive BHs. This type of approach is not new: the standard thin disk paradigm (Shakura & Sunyaev 1973) seems to scale sensibly with mass. The translation of this approach to non-thermal components has not yet been studied. For this Letter, we use the outflow-dominated model of Markoff et al. (2005, hereafter MNW05), with additional modifications as detailed in Maitra et al. (2009). This multi-scale, broadband model has been successfully applied to a variety of BHs at both ends of the mass range individually, but never jointly as we explore here. We emphasize that this test should apply for any model that can address the broadband SEDs of weakly accreting BHs, and thus predict the FP relations.

The details of MNW05 can be found in the above papers, and many applications to both BHBs (see, e.g., Markoff et al. 2005; Gallo et al. 2007; Maitra et al. 2009; Plotkin et al. 2015) and LLAGNs in LINERS (e.g., Markoff et al. 2001, 2008; Maitra et al. 2011; Prieto et al. 2015). Here, we give just a basic summary of the properties of the model and the relevant fitted parameters.

The MNW05 model includes a heuristic, multi-temperature thin disk component (e.g., Shakura & Sunyaev 1973; Mitsuda et al. 1984) whose radius $R_{\rm in}$ and temperature $T_{\rm in}$ are fitted to the data, and whose photons contribute to the photon field for inverse-Compton scattering. Within $r < R_{\rm in}$ we assume that radiatively dominant jets are anchored in a RIAF (see, e.g., Yuan et al. 2002), powered by a fraction of $\dot{M}c^2$ that is divided equally between cold protons and internal pressure (radiating leptons and magnetic fields).

A thermal particle distribution is assumed to enter the jet nozzle, making this region something of an interface with, or proxy for, the inner RIAF/corona. The jet flow solution is based on a self-collimating, freely expanding hydrodynamic wind (see, e.g., Falcke & Biermann 1995; Falcke & Markoff 2000) and thus is decoupled from the internal pressure (see, e.g., Polko et al. 2014 for a relativistic MHD-consistent treatment in development). Thus, once conditions at the launch point are set, the scaling of physical parameters along the jets is fully determined until the location $z_{\rm acc}$. There, a fixed fraction of particles (60%) is accelerated into a power-law distribution with index p and is assumed to be maintained from that point onward by a distributed process as implied by observations (e.g., Jester et al. 2001). There is also an option to inject particles into the jets already accelerated, in which case $z_{\rm acc}$ is not used and a maximum Lorentz factor $\gamma_{\rm max}$ is instead fit to the data. The fitted parameters are: p, $z_{\rm acc}$, $R_{\rm in}$, and $T_{\rm in}$, the scaled power normalization N_j (in units of $L_{\rm Edd}$) injected into the jets at their base, of radius r_0 and height h_0 (sometimes frozen), with a ratio of magnetic to thermal gas pressure k, the temperature of the initial, mildly relativistic Maxwell–Juttner distribution for the radiating particles T_e (which also sets $\gamma_{\rm min}$ for the injected power-law case), and $f_{\rm sc}$, a parameter absorbing uncertainties in the acceleration efficiency when particles are accelerated at $z_{\rm acc}$.

To compare two BHs of different masses requires SEDs of comparable, simultaneous broadband coverage and quality. Currently the only LLAGNs with such extensive coverage are M87 (Prieto et al. 2015), our Galactic center supermassive BH Sgr A*, and M81* from a campaign originally designed to provide a comparison source to Sgr A*. These observations included radio (GMRT, VLA), submillimeter (PdBI, SMA), and X-ray (*Chandra*-HETG), as described by Markoff et al. (2008), where we also showed that the MNW05 model provides a good description of the M81* SED. The fitted parameter ranges were similar to those found in hard state BHBs; however, we were not able to break the degeneracy between two potential origins for the X-ray emission providing statistically comparable fits: direct synchrotron emission from the inner jets or SSC from the jet base/corona.

To study the potential "self-similarity" in mass and attempt to break the above degeneracy, here we seek to compare the SED from M81* to the BHB V404 Cygni (hereafter V404), with masses $7 \times 10^7\,M_\odot$ (Devereux et al. 2003) and $12\,M_\odot$ (Shahbaz et al. 1994), respectively. We use the compiled SED of V404 from Hynes et al. (2009), where the X-ray (*Chandra*-ACIS), UV (*Hubble Space Telescope*, *HST*), and radio data (VLA) were simultaneous, while optical/infrared constraints (e.g., from *Spitzer* and ground-based instruments) were archival. Similarly for M81* we include archival *HST* (IR/UV) and *Spitzer* data, as well as ground-based constraints from *ISO* and MIRLIN (see Markoff et al. 2008 for details). We apply for the first time a multi-zone, multiwavelength model jointly to the data sets from two sources, separated by a huge dynamic range in mass, tying together several model parameters across this mass range. We have developed this new approach within the data analysis software package `ISIS` (Houck & Denicola 2002). Note that scale-free parameters correspond to different physical values; therefore, features in the model SEDs corresponding to, e.g., optical depth, temperature, and cooling breaks will remain dependent on the actual mass of the object. Importantly, the X-ray luminosities of both sources ($L_X/L_{\rm Edd} \equiv \ell_X \sim 10^{-6}$) imply similar $\dot{m}$ (see, e.g., Plotkin et al. 2012), a necessary requirement for this exploration.

2.1. Fitting Methods

Given the complexities of both the data and the spectral model, we did not expect to obtain straightforward fits with a reduced χ^2 value of $\approx$1 using simple Gaussian statistics. We must consider the fact that the error bars in BHBs represent statistical errors on a near-simultaneous measurement, while for

an LLAGN we resolve "waves" of variability at levels of ~20% typical for all bands (e.g., Ho et al. 1999). Such variability would be averaged out over the much shorter BHB timescales (see the discussion in Markoff et al. 2008). Direct comparison of errors across broad energy bands and across mass scales may therefore be less meaningful. Nevertheless, we do require some form of quantitative measure of the quality of the spectral model descriptions, with a means of judging the relative merits of different choices in model assumptions and parameter values. To this end, we have developed exploratory methods to treat the data and perform the fits.

We are concerned with both the relative flux normalizations and statistical weighting of individual observational bands. As differences can arise from cross-calibration uncertainties, we allow for the usual fitted constant between spectra from different X-ray satellites (see Plucinsky et al. 2012). To account for delays among energy bands and the lack of strict simultaneity among the observations, as well as allowing for systematic uncertainties between instruments in different energy bands, we further adopt fractional, as opposed to statistical, error bars for the non-X-ray data. For V404, we replace the non-X-ray statistical error bars with 5% fractional error bars. (Larger error bars resulted in the few radio points exerting too little statistical influence over the fits, smaller error bars resulted in larger fit statistics regardless of fit parameters.) For M81*, we replace the non-X-ray statistical error bars with 15% fractional error bars (i.e., comparable to the intrinsic radio variability), except for the non-simultaneous IR/UV spectra where we adopt 40% fractional error bars. For the UV data, there is some debate whether these are detections of the emission from M81* or are merely upper limits to the central object emission (e.g., Maoz et al. 2005). Adopting these large error bars thus allows the *HST* and other non-simultaneous data to influence, but not dominate, the model fits and act as upper limits. These choices admittedly contain a degree of subjective judgement. "Best practices" for combining data sets from multiple, independent instruments remains an area of active research, with some promising Bayesian methods allowing a more formal approach for including priors for instrument systematics (see, e.g., Anderson et al. 2015). The focus of this work is to first gauge whether tying parameters across such a large mass range in these independent sources offers any viable solutions, with future work devoted to refining parameter estimates of these models.

To fit the spectra, we begin with the usual approach of minimizing χ^2 with a fast algorithm, but we then extensively explore parameter space via the use of an `ISIS` implementation (described in detail in Murphy & Nowak 2014) of the Markov Chain Monte Carlo (MCMC) method of Foreman-Mackey et al. (2013) and Goodman & Weare (2010). Parameter space is explored via 510 trial "walkers" that are evolved over a series of 3000 steps, only the last 1000 of which are retained. The resulting multi-dimensional distribution of 5.4×10^5 parameter values are used to create one- and two-dimensional histograms that then yield parameter error bars and confidence contours. The parameter set for the lowest χ^2 value found anywhere in this process is taken as the best-fit model.

We start with the best-fit parameters for the two degenerate classes of models (synchrotron versus SSC-dominated) fit to M81* from Markoff et al. (2008). We then explore joint fits to the M81* and V404 spectra, where we tie values of various parameter subsets for the two sources. As the values T_e, $T_{\rm in}$, and $f_{\rm sc}$ are the most obviously affected by local physical conditions, these particular parameters are never tied. Instead, we explore joint fits where different subsets of the direct mass-scaling parameters, r_0, $z_{\rm acc}$, $r_{\rm in}$, are tied. We further explore tying additional physical parameters, namely, p and k, that fall within small ranges in prior studies of individual sources across the mass range.

3. RESULTS

In Table 1, we list the model parameters for the best fits shown in Figure 1, distinguishing between those free to vary for each source and those tied together for a joint fit to both SEDs.

The synchrotron-dominated scenario is clearly the most successful, providing a surprisingly good fit to both sources with almost half the parameters tied—including all relevant physical scales. In contrast, no SSC-dominated scenario could fit both sources in a scalable way. While this result does not rule out SSC-dominated scenarios, the idea that these two sources fall on the FP at similar Eddington fractions but via completely different emission mechanisms seems less likely. Even when decoupling some of the tied parameters, we failed to find substantially improved fits. Given that the synchrotron scenario not only had the best χ^2, but also allowed for the greatest number of tied parameters, we favor the interpretation that synchrotron emission drives the FP correlation for at least the range $\ell_X \sim 10^{-7}$–10^{-6}.

Compared to the best individual fits to M81* (Markoff et al. 2008), several parameters do not coincide within the errors to those found here. Specifically, the joint fitting technique selects a slightly hotter plasma injected within a larger jet base and a slightly steeper injected power law. There are several potential reasons for this difference, including the possibility that the earlier fits were a local rather than a global minimum since they were not obtained with an MCMC approach. It is worth noting that the M81*/V404 observations are close to, but not exactly at, the same $\dot{m}$. The individual data sets are also not fully simultaneous. Ultimately, one would prefer to repeat this experiment with fully simultaneous data sets at exactly the same ℓ_X. On the other hand, the best-fit parameter values still fall well within the ranges found from earlier modeling of many individual sources. Thus, this new joint fitting approach does not fundamentally change our ideas about the source physics or geometry, but rather serves as a promising method to break the degeneracy between emission scenarios.

The advantage of the MCMC approach is that with the multi-dimensional probability distribution we can a posteriori explore all 120 possible two-parameter correlations. This allows a new level of insight into physical drivers of the FP as well as pinpointing model degeneracy that needs to be addressed in future work. We find that the parameters for the synchrotron model have well-determined means and errors as derived from their one-dimensional histograms. When examining two-dimensional histograms, only a few parameters showed any degree of correlation (see Figure 2). Several of these (not shown) are commonly seen from fits to similar sources, e.g., correlations between fitted neutral column and parameters affecting spectral slope. Likewise for M81*, there is a correlation between disk radius and temperature, indicating that although a soft excess is required by the data, its detailed properties are not well determined. Figure 2 shows the 68%, 90%, and 99% confidence

Table 1
Fit Parameters for Synchrotron-dominated and Compton-dominated Fits

Source	N_H (10^{21} cm^{-2})	N_j (10^{-5})	T_{in} (10^4 K)	T_e (10^{11} K)	h_0 (r_0)	f_{sc} (10^{-4})	γ_{max} (10^2)	p	k	r_{in}	r_0 (GM/c^2)	z_{sh}	χ^2_ν/dof
M81*	$0.31^{+0.11}_{-0.03}$	$0.36^{+0.05}_{-0.04}$	$1.6^{+0.3}_{-1.3}$	$16.6^{+1.6}_{-0.7}$	5[a]	47^{+8}_{-12}	…	…	…	…	…	…	…
V404	8.8[a]	17^{+20}_{-5}	106^{+5}_{-37}	$0.09^{+0.02}_{-0.02}$	1.5[a]	$0.8^{+0.7}_{-0.2}$	…	…	…	…	…	…	…
Joint	…	…	…	…	…	…	…	$2.74^{+0.05}_{-0.01}$	$0.73^{+0.53}_{-0.07}$	$1.1^{+8.7}_{-0.1}$	65^{+10}_{-3}	305^{+15}_{-21}	1257/582
M81*	$0.03^{+0.02}_{-0.01}$	$0.30^{+0.06}_{-0.04}$	$0.07^{+0.49}_{-0.02}$	$2.1^{+0.3}_{-0.3}$	…	…	15^{+20}_{-7}	$3.22^{+0.10}_{-0.13}$	$0.45^{+0.48}_{-0.15}$	…	…	…	…
[a]	$0.65^{+0.31}_{-0.03}$	112^{+8}_{-11}	$0.35^{+0.09}_{-0.05}$	…	…	$0.22^{+0.09}_{-0.08}$	$2.47^{+1.28}_{-0.36}$	$0.32^{+0.28}_{-0.02}$	…	…	…	…	
Joint	…	…	…	…	$10.1^{+5.3}_{-0.1}$	…	…	…	…	$1.1^{+3.1}_{-0.1}$	$3.7^{+1.5}_{-0.1}$	…	2671/582

Notes. Fit parameters for the synchrotron-dominated (top) and SSC-dominated (bottom) fits. The model components are: blackbody emission from the accretion disk and/or star (magenta/dotted), thermal synchrotron (light green/dashed), post-accelerated non-thermal synchrotron (dark green/solid), inverse-Compton/SSC (orange/dashed–dotted). Note that in the SSC-dominated fit, accelerated particles were injected at the base, thus z_{acc} and f_{sc} are not used, while γ_{max} is. These parameters gave the lowest χ^2 values for all parameter space explored, while error bars are the bounds that encompass 90% of the one-dimensional parameter histograms obtained from MCMC exploration of the model fit (see the text). Other fixed physical parameters: mass (M81: $7 \times 10^7\ M_\odot$, V404: $12\ M_\odot$), distance (M81: 3.6 Mpc, V404: 2.4 kpc), inclination (M81: 20°, V404: 56°); see Markoff et al. (2008) and Hynes et al. (2009).
[a] Frozen parameter.

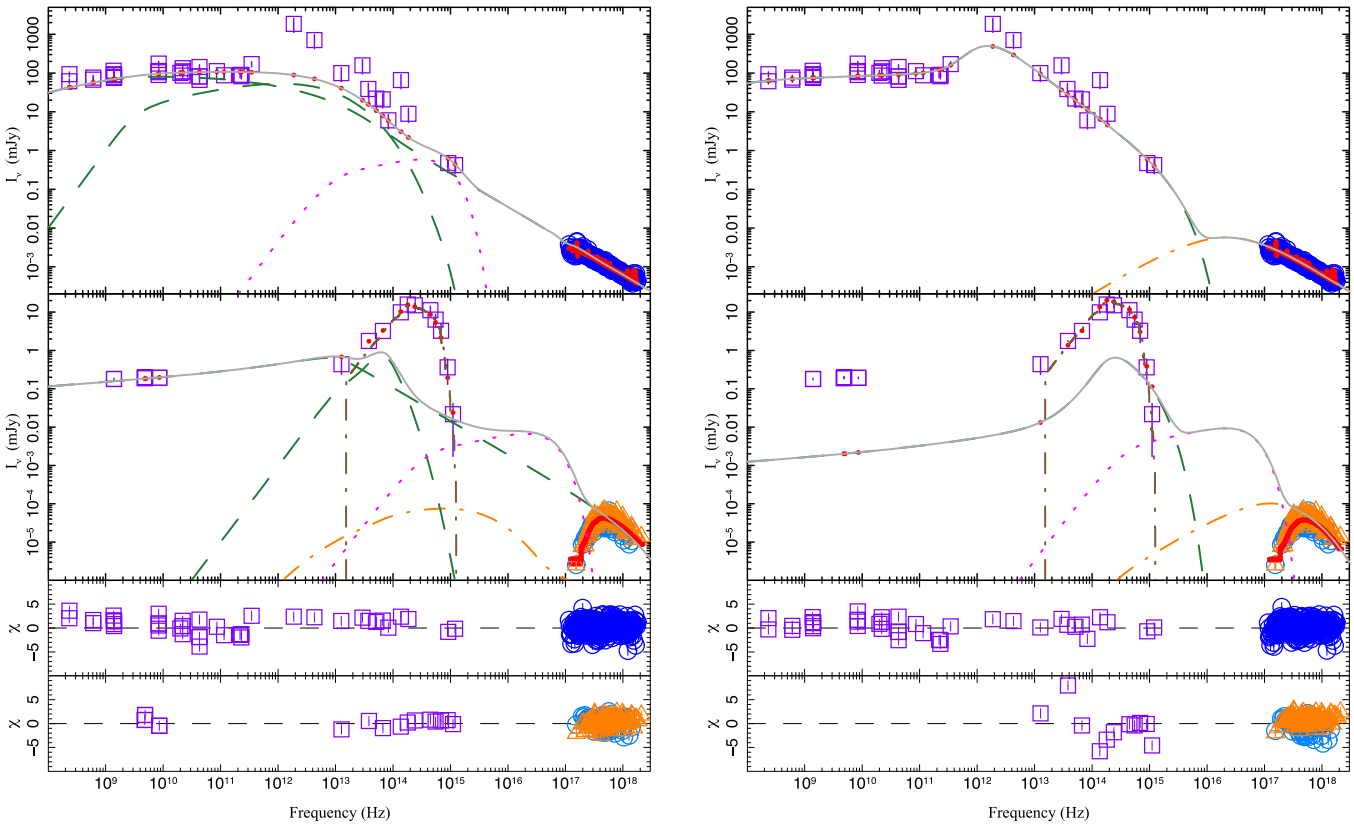

Figure 1. Best-fit synchrotron-dominated model (left) and synchrotron self-Compton-dominated model (right). The top panels are the flux-corrected spectra for M81*, while the panels below are the V404 flux-corrected spectra, and the bottom panels show the fit residuals. Lines show the individual model components (light green/dashed: thermal synchrotron, dark green/dashed: non-thermal synchrotron, orange/dashed–dotted: synchrotron self-Compton, magenta/dotted: multicolor blackbody disk, and gray/dashed–dotted: stellar component in the case of V404), all absent absorption. The gray/solid line shows the total model, while the red/solid line and dots show the model after forward folding through detector space, including absorption.

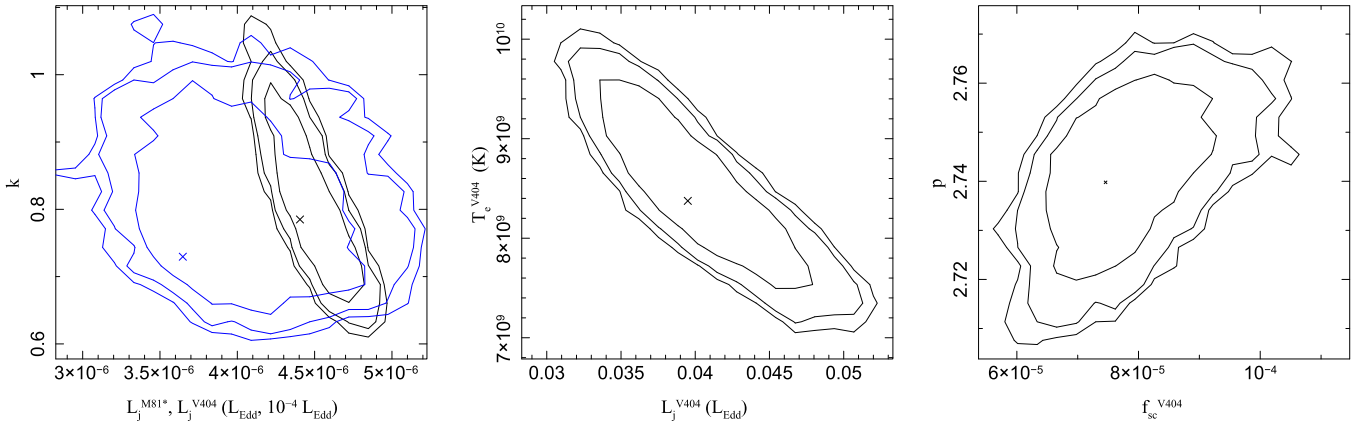

Figure 2. The significant two-parameter correlations found via our MCMC exploration of parameter space for the synchrotron-dominated fits. Left: equipartition parameter k (tied for both sources) vs. scaled injected jet power, N_j (renormalized by 10^{-4} for V404). Middle: coronal temperature, T_e, vs. scaled injected jet power for V404. Right: power-law slope, p, of accelerated particle distribution (tied for both sources) vs. the plasma particle acceleration timescale parameter, $f_{\rm sc}$, for V404.

contours from all two-dimensional histograms where we see interesting correlations, indicating either a physical relation or model degeneracy between these parameters. Both sources show a correlation (stronger for V404) between the normalization power N_j and the equipartition parameter k. This correlation indicates degeneracy in how the injected power is divided between the radiating particles and the magnetic field. As k is increased, putting more energy into the magnetic fields, respectively, fewer electrons are required for the same spectral fit, resulting in somewhat lower power. Fewer electrons can provide the same energy density with a higher temperature, thus giving the correlation seen in the middle panel. Taken together, these two figures indicate a degeneracy between N_j, k, and T_e in the model due to the parameterization of the energy partition at the base of the jets. The rightmost panel shows a similar degeneracy between the particle power-law index and $f_{\rm sc}$ on which the power-law cutoff depends. A harder value of p can compensate for a lower cutoff up to a point.

4. DISCUSSION AND CONCLUSIONS

Our results support an emerging paradigm that the weakly accreting BHs populating the fundamental plane can be treated as self-similar objects, whose physical behavior is determined by accretion properties rather than mass. Specifically, we show that two BHs, separated by seven orders of magnitude in mass but with comparable ℓ_X, can be statistically described as "self-similar" in the physical scale (in units of r_g). For the more successful synchrotron-dominated model, two additional parameters can also be tied: the power-law distribution p, often thought to be universal for a given acceleration process, and k, the partition of energy density between magnetic fields and radiating particles. The fact that k is roughly consistent with unity suggests that this parameter could be eliminated with the assumption of equipartition. The best value for p could imply either weak acceleration efficiency or very efficient accelerations (such as from reconnection; e.g., Sironi & Spitkovsky 2014) in a cooling-dominated regime. The SSC-dominated scenario does not achieve a good description of the data, even with several additional parameters allowed to vary. Interestingly, independent works suggest an interplay exists between synchrotron and SSC as a function of $\dot{m}$, consistent with our results. For example, Russell et al. (2010) empirically show that synchrotron emission dominates the X-ray band around $L_{\rm bol} \sim 10^{-4}$–10^{-3}, while fits to LLAGNs below $L_X \sim 10^{-7} L_{\rm Edd}$ seem to prefer SSC radiation (Markoff et al. 2001; Plotkin et al. 2015; Prieto et al. 2015). The FP slope does not seem to change despite this apparent transition (Corbel et al. 2013; Gallo et al. 2014), although the spectral index does show softening below $\ell_X \sim 10^{-5}$ (Plotkin et al. 2013).

The results of our study suggest that it is possible to exploit mass scaling to break the longstanding degeneracies between the model classes that persist for AGNs (see, e.g., Harris & Krawczynski 2006) as well as BHBs (e.g., Nowak et al. 2011). Compared to individual fitting, the correlations found between parameters pinpoint the interplay between parameter values due to model degeneracies as well as probing meaningful physical relationships and the partition of energy between magnetic, thermal, and kinetic. This new method thus opens the door to several useful applications, such as using BHBs to infer conditions in obscured regions deep in the hearts of galactic nuclei or to study processes that affect galaxy evolution over cosmological timescales.

Using mass scaling for simultaneous joint/multiple fitting also has the potential to constrain the SEDs of BHs with only sparse data coverage, as well as better pegging the contribution of weak accretion activity, particularly in the millimeter/submillimeter band of nearby galaxies. For instance, the discrepancy between the model and data in the submillimeter/OIR regime in Figure 1 is expected due to galactic stellar and dust contributions (e.g., Bendo et al. 2010). We therefore plan to apply this new method to a larger sample of LLAGNs with sub-arcsecond aperture constraints on the galactic component (e.g., Mason et al. 2012; Fernández-Ontiveros et al. 2013) in future work.

Finally, a deeper understanding of why mass-scaling holds will elucidate the respective roles of outer boundary conditions versus intrinsic accretion flow physics, guiding the way toward more reliable prescriptions of BH feedback.

S.M. is grateful to the University of Texas in Austin for its support through a Tinsley Centennial Visiting Professorship.

REFERENCES

Anderson, B., Chiang, J., Cohen-Tanugi, J., et al. 2015, arXiv:1502.03081
Belloni, T. M. 2010, in Lecture Notes in Physics, Vol. 794, ed. T. Belloni (Berlin: Springer), 53
Bendo, G. J., Wilson, C. D., Pohlen, M., et al. 2010, A&A, 518, L65
Blandford, R. D., & Königl, A. 1979, ApJ, 232, 34
Corbel, S., Coriat, M., Brocksopp, C., et al. 2013, MNRAS, 428, 2500
Devereux, N., Ford, H., Tsvetanov, Z., & Jacoby, G. 2003, AJ, 125, 1226
Falcke, H., & Biermann, P. L. 1995, A&A, 293, 665
Falcke, H., Körding, E., & Markoff, S. 2004, A&A, 414, 895
Falcke, H., & Markoff, S. 2000, A&A, 362, 113
Fender, R. P. 2001, MNRAS, 322, 31
Fernández-Ontiveros, J. A., Almudena Prieto, M., Acosta-Pulido, J. A., Markoff, S., & González-Martín, O. 2013, in European Physical Journal Web of Conf., 61, The Innermost Regions of Relativistic Jets and Their Magnetic Fields, ed. J. L. Gómez (Granada: EPJ), 4005
Foreman-Mackey, D., Hogg, D. W., Lang, D., & Goodman, J. 2013, PASP, 125, 306
Gallo, E., Migliari, S., Markoff, S., et al. 2007, ApJ, 670, 600
Gallo, E., Miller-Jones, J. C. A., Russell, D. M., et al. 2014, MNRAS, 445, 290
Goodman, J., & Weare, J. 2010, CAMCS, 5, 65
Gültekin, K., Cackett, E. M., Miller, J. M., et al. 2009, ApJ, 706, 404
Harris, D. E., & Krawczynski, H. 2006, ARA&A, 44, 463
Heinz, S., & Sunyaev, R. A. 2003, MNRAS, 343, L59
Ho, L. C., van Dyk, S. D., Pooley, G. G., Sramek, R. A., & Weiler, K. W. 1999, AJ, 118, 843
Houck, J. C., & Denicola, L. A. 2002, in ASP Conf. Series 216, Astronomical Data Analysis Software and Systems IX (San Francisco, CA: ASP), 591
Hynes, R. I., Bradley, C. K., Rupen, M., et al. 2009, MNRAS, 399, 2239
Jester, S., Röser, H.-J., Meisenheimer, K., Perley, R., & Conway, R. 2001, A&A, 373, 447
Körding, E., Falcke, H., & Corbel, S. 2006a, A&A, 456, 439
Körding, E. G., Jester, S., & Fender, R. 2006b, MNRAS, 372, 1366
Maitra, D., Markoff, S., Brocksopp, C., et al. 2009, MNRAS, 398, 1638
Maitra, D., Miller, J. M., Markoff, S., & King, A. 2011, ApJ, 735, 107
Maoz, D., Nagar, N. M., Falcke, H., & Wilson, A. S. 2005, ApJ, 625, 699
Markoff, S. 2010, in Lecture Notes in Physics, Vol. 794, ed. T. Belloni (Berlin: Springer), 143
Markoff, S., Falcke, H., Yuan, F., & Biermann, P. L. 2001, A&A, 379, L13
Markoff, S., Nowak, M., Corbel, S., Fender, R., & Falcke, H. 2003, A&A, 397, 645
Markoff, S., Nowak, M., Young, A., et al. 2008, ApJ, 681, 905
Markoff, S., Nowak, M. A., & Wilms, J. 2005, ApJ, 635, 1203
Mason, R. E., Lopez-Rodriguez, E., Packham, C., et al. 2012, AJ, 144, 11
McClintock, J. E., & Remillard, R. A. 2006, in Compact Stellar X-Ray Sources (Cambridge: Cambridge Univ. Press), 157
McHardy, I. M., Arévalo, P., Uttley, P., et al. 2007, MNRAS, 382, 985
McHardy, I. M., Koerding, E., Knigge, C., Uttley, P., & Fender, R. P. 2006, Natur, 444, 730
Merloni, A., Heinz, S., & di Matteo, T. 2003, MNRAS, 345, 1057
Mitsuda, K., Inoue, H., Koyama, K., et al. 1984, PASJ, 36, 741
Murphy, K. D., & Nowak, M. A. 2014, ApJ, 797, 12
Narayan, R., & Yi, I. 1994, ApJL, 428, L13
Nowak, M. A., Hanke, M., Trowbridge, S. N., et al. 2011, ApJ, 728, 13
Plotkin, R. M., Gallo, E., & Jonker, P. G. 2013, ApJ, 773, 59
Plotkin, R. M., Gallo, E., Markoff, S., et al. 2015, MNRAS, 446, 4098
Plotkin, R. M., Markoff, S., Kelly, B. C., Körding, E., & Anderson, S. F. 2012, MNRAS, 419, 267
Plucinsky, P. P., Beardmore, A. P., DePasquale, J. M., et al. 2012, Proc. SPIE, 8443, 12
Polko, P., Meier, D. L., & Markoff, S. 2014, MNRAS, 438, 959
Prieto, M. A., Fernández-Ontiveros, J., Markoff, S., Espada, D., & González-Martín, O. 2015, MNRAS, submitted (arXiv:1508.02302)
Russell, D. M., Maitra, D., Dunn, R. J. H., & Markoff, S. 2010, MNRAS, 405, 1759
Shahbaz, T., Ringwald, F. A., Bunn, J. C., et al. 1994, MNRAS, 271, L10
Shakura, N. I., & Sunyaev, R. A. 1973, A&A, 24, 337
Sironi, L., & Spitkovsky, A. 2014, ApJL, 783, L21
Yuan, F., Cui, W., & Narayan, R. 2005, ApJ, 620, 905
Yuan, F., Markoff, S., & Falcke, H. 2002, A&A, 383, 854
Yuan, F., Quataert, E., & Narayan, R. 2003, ApJ, 598, 301